First-Row Transition Metal Bis(amidinate) Complexes; Planar Four-Coordination of Fe^{II} Enforced by Sterically Demanding Aryl Substituents

Christian A. Nijhuis,[a] Erica Jellema,[a] Timo J. J. Sciarone,[a] Auke Meetsma,[a] Peter H. M. Budzelaar,[b] and Bart Hessen*[a]

Keywords: Transition metals / Solid-state structures / Ligand effects / Amidinate / Density functional calculations

The sterically hindered benzamidinate ligand $[PhC(NAr)_2]^-$ (Ar = 2,6-*i*$Pr_2C_6H_3$) has been employed to prepare bis(amidinate) complexes $[\{PhC(NAr)_2\}_2M]$ of the divalent first-row transition metals Cr–Ni (**1**–**5**). For Cr (planar), Mn and Co (tetrahedral) the observed structures follow the electronic preference for the metal ion in its highest spin multiplicity, as determined by DFT calculations. Remarkably, the Fe derivative adopts a distorted planar structure while retaining the high-spin (S = 2) configuration. This rare combination is due to reduced interligand steric interactions in the planar vs. the tetrahedral structure, combined with a relatively small electronic preference of Fe^{II} for the tetrahedral environment. Thus, the simple bidentate ligand *N*,*N*′-diarylbenzamidinate provides a convenient means to make this unusual species accessible for further study.

Introduction

Amidinate anions, with general formula $[R'NC(R)NR'']^-$, have been employed widely as ligands in transition metal and in main group chemistry.[1,2] Their steric and electronic properties are readily modified through variation of the substituents on the carbon and nitrogen atoms, and they have been employed as ancillary ligands in various catalytic conversions, e.g. oligomerisation[3,4] or polymerisation[5–20] of olefins or of cyclic esters.[21,22] Due to the geometric constraints of the NCN ligand backbone, amidinates have small N–M–N bite angles (typically 63–65°). They have a rich coordination geometry in which both chelating and bridging coordination modes can be achieved. The latter has allowed the synthesis of a range of dinuclear complexes with short metal–metal separations.[23–34] The balance between chelating and bridging coordination is critically governed by the substitution pattern of the amidinate ligand. Steric interactions between the substituents on the carbon and nitrogen atoms influence the orientation of the nitrogen lone pairs. Large substituents on the carbon atom induce a convergent orientation of the lone pairs (favouring chelation), while small substituents lead to a more parallel orientation of the lone pairs (enabling bridging).[34,35]

The substituents on the amidinate nitrogen atoms can be used to tune the steric demand of the ligand, influencing the coordination geometry of the metal centre in bis(amidinate) complexes with chelating amidinate ligands. Thus, Winter et al. have demonstrated that an increase in steric demand of the alkyl substituent R in $[\{MeC(NR_2)\}_2Cr]$ from R = *i*Pr to *t*Bu results in a change from square-planar to tetrahedral coordination of the high-spin Cr^{II} centre.[36] For R = *t*Bu, interligand steric interactions apparently become dominant over an electronic preference for square-planar coordination.[37]

The steric hindrance imparted by alkyl substituents on the amidinate nitrogen atoms has its main effect in the NMN coordination plane. To effect steric shielding above and below this coordination plane, two approaches are possible. Introduction of a terphenyl substituent on the amidinate backbone *carbon* atom provides such shielding (as shown by Arnold et al. in complexes of Li^I, Mg^{II}, Al^{III}, Y^{III} and a series of first-row transition metals),[38–43] but relatively remote from the metal–ligand bonds. Another approach is the use of *ortho*-disubstituted aryl groups on the *nitrogen* atoms. By virtue of the perpendicular orientation of the aryl moieties with respect to the NCN backbone (especially when relatively large substituents on the carbon atom are used), the *ortho* substituents provide steric protection to the sites above and below the coordination plane. The 2,6-(diisopropyl)phenyl group (Ar = 2,6-*i*$Pr_2C_6H_3$) has proven to be very efficient in this respect, and has been used successfully in the development of late transition metal olefin polymerisation catalysts with neutral diimine li-

[a] Dutch Polymer Institute, Center for Catalytic Olefin Polymerisation, Stratingh Institute for Chemistry and Chemical Engineering, University of Groningen,
Nijenborgh 4, 9747 AG Groningen, Netherlands
Fax: +31-50-363-4315
E-mail: hessen@chem.rug.nl
[b] Dutch Polymer Institute, Institute for Molecules and Materials, Metal-Organic Chemistry, Radboud University Nijmegen,
P. O. Box 9010, 6500 GL Nijmegen, Netherlands
Fax: +31-24-355-3450
E-mail: p.budzelaar@science.ru.nl

Supporting information for this article is available on the WWW under http://www.eurjic.org or from the author.

gands[44–47] and in the synthesis of low-coordinate, electron-deficient metal complexes stabilised by β-diketiminates.[48] With amidinate ligands, these substituents have been used only sparingly thus far. The amidines $[RC(NAr)_2]H$ (R = CH_3, 4-MeC_6H_4, 4-$MeOC_6H_4$) were synthesised by Boeré et al., who also reported some initial studies of their Mo^0 coordination chemistry.[49] The amidinates $[tBuC(NAr)_2]^-$, $[4\text{-}MeC_6H_4C(NAr)_2]^-$ and $[PhC(NAr)_2]^-$ have been used as ligands for Al^{III},[50] Ni^{II},[7] group 3 and lanthanide metals.[9,20,22] Due to the positioning of the steric hindrance of these ligands, interesting interligand steric interactions may be anticipated when two of these ligands are attached to (relatively small) first-row transition metals.

Bis(amidinate) complexes of the divalent first-row transition metal ions have been found to adopt either a (distorted) tetrahedral or a (distorted) square-planar geometry. The former is observed for bis(amidinates) complexes of Mn^{II}–Co^{II},[41,51–54] while for bis(amidinate) complexes of Cr^{II} and Ni^{II} both types of geometry have been found to occur.[34,36,41,55–58] In this paper we describe the synthesis and characterisation of the bis(benzamidinate) complexes $[\{PhC(NAr)_2\}M]$ (M = Cr–Ni, Ar = 2,6-$iPr_2C_6H_3$, Figure 1). Interligand interactions between the sterically demanding amidinate ligands are found to enforce a distorted square-planar geometry onto high-spin Fe^{II}, which is exceptional for this ion when bound to two bidentate ligands.

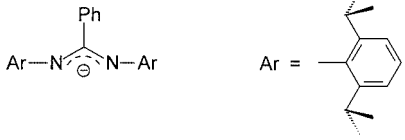

Figure 1. *N*,*N*′-Bis(2,6-diisopropylphenyl)benzamidinate

Results and Discussion

Synthesis

The bis(amidinate) complexes $[\{PhC(NAr)_2\}_2M]$ [M = Cr (**1**), Mn (**2**), Fe (**3**), Co (**4**)] were obtained by reaction of the anhydrous metal chlorides with the lithium amidinate $Li[PhC(NAr)_2]$ (Scheme 1). The latter was generated in situ by deprotonation of the amidine by *n*BuLi in THF. The products were isolated by extraction with hexanes or pentane and crystallisation from the same solvents, affording the air-sensitive, crystalline bis(amidinate) complexes in 48 (**2**) to 91% (**3**) isolated yield. The Ni complex $[\{PhC(NAr)_2\}_2Ni]$ (**5**) was prepared from the lithium amidinate and $[(DME)NiBr_2]$. This complex was obtained in 47% yield after crystallisation from toluene.

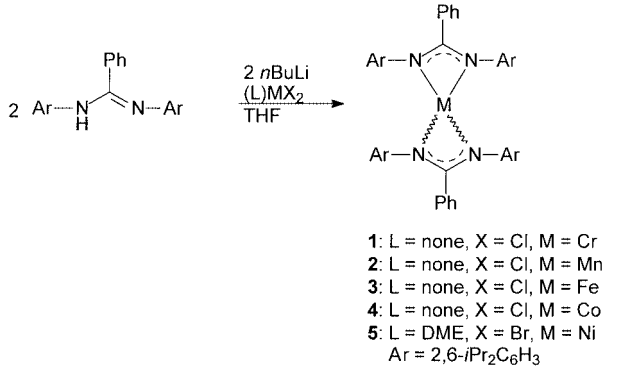

Scheme 1.

The complexes were characterised by elemental analysis, X-ray diffraction, ^1H NMR and IR spectroscopy and solid-state variable-temperature magnetic susceptibility measurements.

Molecular Structures

The molecular structures of the bis(amidinate) complexes were determined by single-crystal X-ray diffraction. Geometric parameters for the structures displayed in Figure 2 are given in Table 1.

All structures show symmetric, chelating coordination of the amidinate ligands with the aryl and phenyl substituents making angles of 61–86° (Ar) and 23–51° (Ph) with the N–M–N coordination planes. The C–N bonds in the amidinate backbones do not differ significantly in length and the nitrogen atoms deviate only slightly from planarity ($\Sigma_{\angle N}$ = 354–360°), suggesting full electron delocalisation in the NCN framework. The bite angle of the ligand is restricted to 64–69° by the geometry of the amidinate backbone.

The Mn and Co complexes **2** and **4** are best described as distorted tetrahedral, in which the NMN coordination planes of the two amidinate ligands are inclined at 74.18(15)° (Mn) and 69.5(4)° (Co), respectively. The average bite angles in the Mn complex (63.59°) are ca. 2° smaller than those in the Co analogue (66.3°) reflecting the smaller ionic radius of the latter metal ion.[59] Consistently, the M–N distances in the Mn^{II} complex are ca. 0.1 Å longer than in the and Co^{II} derivative.

The Cr and Ni complexes **1** and **5** show a distorted planar arrangement of the four coordinating nitrogen atoms. For bis(amidinate) derivatives of Cr^{II}, this coordination geometry is commonly observed,[34,36,57] but planar coordination in Ni^{II} bis(amidinates) is less common, the only example being the complex $[\{PhC(NXyl)(NSiMe_3)\}_2Ni]$ (Xyl = 2,6-$Me_2C_6H_3$) reported recently by Lee et al.[56] The amidinate NMN coordination planes are inclined at 7.73(10)° (Cr) and 4.13(13)° (Ni), respectively. The average bite angles in the Cr complex are approximately 4° smaller than in the Ni complex, consistent with the smaller ionic radius for square planar Ni^{II}.[59] The same trend is observed in the M–N bond lengths, which are significantly shorter for the Ni derivative.

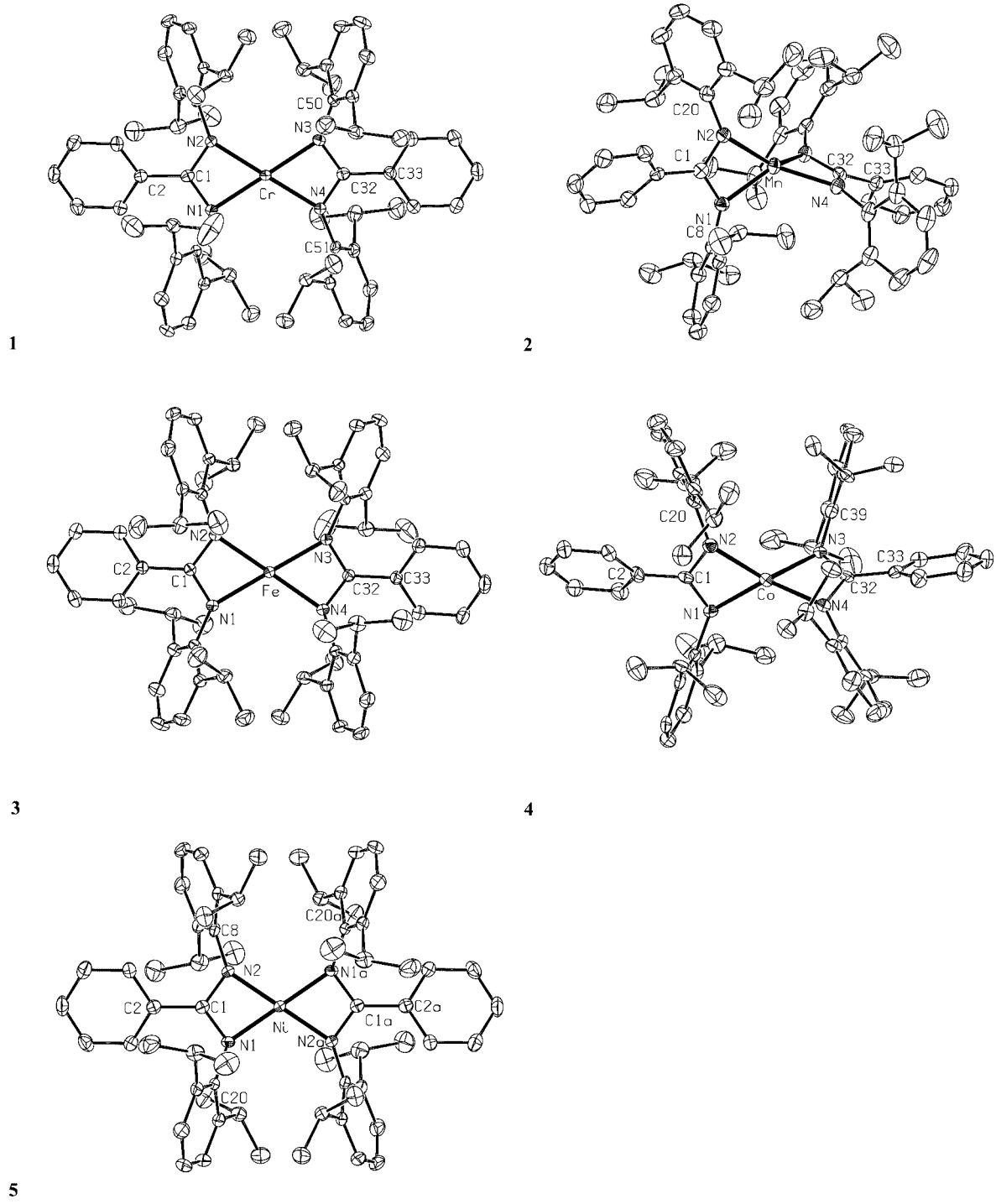

Figure 2. Molecular structures of complexes [{PhC(NAr)$_2$}$_2$M] (**1–5**) (50% ellipsoids). Hydrogen atoms and cocrystallised solvent molecules have been omitted for clarity.

Surprisingly, the Fe complex **3** is also found to adopt a distorted-planar coordination geometry. The angle between the two NMN coordination planes of 12.37(8)° is slightly larger than for the Cr and Ni analogues, but still warrants a description of **3** as a distorted planar structure. The planar coordination geometry in **3** is in sharp contrast to the other homoleptic bis(amidinate) complexes of Fe^{II},[51–54] which are exclusively tetrahedral. Planar structures for Fe^{II} are commonly found with (macrocyclic) tetradentate donor ligands, which are preorganised for this geometry.[60,61] Examples include salen [salen = *N*,*N*′-ethylenebis(salicylideneimine)],[62] calix[4]arene,[63] porphyrins,[64,65] phthalocyanines[66–69] and a number of macrocyclic bis(β-diiminato) ligands.[70–73] Planar coordination of Fe^{II} by two bidentate

Table 1. Selected bond lengths and angles for bis(amidinate) complexes [{PhC(NAr)$_2$}$_2$M].

Distances [Å]	Cr (**1**)	Mn (**2**)	Fe (**3**)	Co (**4**)	Ni (**5**)[a]
M–N1	2.0577(16)	2.111(3)	2.0662(14)	1.989(7)	1.918(2)
M–N2	2.0546(18)	2.118(3)	2.0532(16)	2.029(6)	1.9288(18)
M–N3	2.0575(16)	2.101(3)	2.0639(12)	1.998(7)	1.918(2)
M–N4	2.0583(18)	2.123(3)	2.0528(16)	2.012(6)	1.9288(18)
N1–C1	1.340(3)	1.343(4)	1.335(2)	1.317(10)	1.344(3)
N2–C1	1.344(2)	1.336(4)	1.338(2)	1.342(12)	1.338(3)
N3–C32	1.343(3)	1.340(4)	1.336(2)	1.322(9)	1.344(3)
N4–C32	1.345(2)	1.323(4)	1.338(2)	1.346(11)	1.338(3)
Angles(°)					
N1–M–N2	64.87(7)	63.55(9)	65.06(6)	66.2(3)	68.63(8)
N1–M–N3	177.08(6)	133.73(10)	174.93(5)	140.4(3)	177.12(8)
N1–M–N4	115.70(7)	125.83(10)	114.72(6)	129.3(3)	111.42(8)
N2–M–N3	114.71(7)	132.3(1)	116.11(5)	123.7(3)	111.42(8)
N2–M–N4	174.69(6)	152.41(10)	171.86(5)	146.8(2)	178.29(9)
N3–M–N4	65.00(7)	63.63(9)	64.90(5)	66.4(3)	68.63(8)
M–N1–C1	92.25(11)	92.00(19)	91.25(10)	92.4(6)	91.88(15)
M–N1–C8	141.74(14)	140.4(2)	142.12(12)	140.2(5)	138.35(16)
C1–N1–C8	123.99(17)	123.2(3)	124.56(15)	124.7(7)	124.0(2)
M–N2–C1	92.27(13)	91.92(19)	91.75(11)	89.9(4)	91.57(14)
M–N2–C20	138.69(13)	141.3(2)	141.81(11)	142.9(6)	139.36(18)
C1–N2–C20	124.91(17)	124.7(3)	124.49(15)	123.9(6)	124.5(2)
M–N3–C32	92.20(11)	91.55(18)	91.59(9)	92.0(5)	91.88(15)
M–N3–C39	140.60(14)	143.2(2)	142.69(11)	137.6(5)	138.35(16)
C32–N3–C39	124.11(17)	121.5(3)	124.50(13)	124.8(7)	124.0(2)
M–N4–C32	92.09(13)	91.08(19)	92.03(11)	90.7(4)	91.57(14)
M–N4–C51	141.20(13)	143.6(2)	140.03(11)	143.1(6)	139.36(18)
C32–N4–C51	123.91(17)	123.7(3)	125.18(15)	124.8(6)	124.5(2)
N1–C1–N2	110.52(17)	112.5(3)	111.93(15)	111.2(7)	107.9(2)
N1–C1–C2	124.97(17)	122.4(3)	124.08(14)	124.5(8)	125.7(2)
N2–C1–C2	124.49(19)	125.2(3)	123.99(16)	124.3(7)	126.4(2)
N3–C32–N4	110.69(17)	113.5(3)	111.42(14)	110.7(7)	107.9(2)
N3–C32–C33	124.66(17)	122.6(3)	124.51(14)	124.8(8)	125.7(2)
N4–C32–C33	124.64(18)	123.8(3)	124.06(15)	124.4(7)	126.4(2)

[a] For ease of comparison, the atoms of the Ni complex (**5**) have been labelled here in analogous fashion to that in the other complexes, in spite of its crystallographic C_2 symmetry (N1_a → N3, N2_a → N4, C1_a → C32 etc.).

ligands is exceptional, although some bis(dithiolato)Fe^{II} dianions have been structurally characterised as distorted square-planar.[74,75]

A prominent feature of the complexes with the planar structure, **1**, **3** and **5**, is that the Ar substituents are all tilted relative to the coordination plane to minimise interligand repulsion by interlocking the *i*Pr substituents. This imparts to these compounds an approximate D_2 symmetry. It is seen by NMR spectroscopy that this behaviour is also present in solution (vide infra).

Magnetic Properties

Except for the diamagnetic Ni derivative **5**, all the bis(amidinate) derivatives reported here are paramagnetic. Variable-temperature magnetic susceptibility measurements were performed on crystalline samples of **1**–**4**. In view of the low symmetry of the complexes, *d*-orbital degeneracy is expected to be largely removed, thus quenching most orbital contributions to the ground state. Normal Curie–Weiss behaviour is therefore anticipated. Indeed, plots of χ^{-1} vs. T in the range 25–300 K (Figure 3) show good linear correlation for the Cr, Mn and Fe complexes with θ = –2.3, –1.3 and 2.5 K, respectively. For the Co derivative **4** a departure from the Curie–Weiss law is seen at elevated temperatures. This behaviour indicates the presence of a temperature-independent paramagnetism (TIP) contribution, which is not unusual for tetrahedral Co^{II}.[76] Over the temperature range of 25–175 K, the susceptibility of **4** can be described by Curie–Weiss behaviour with θ = –5.6 K.

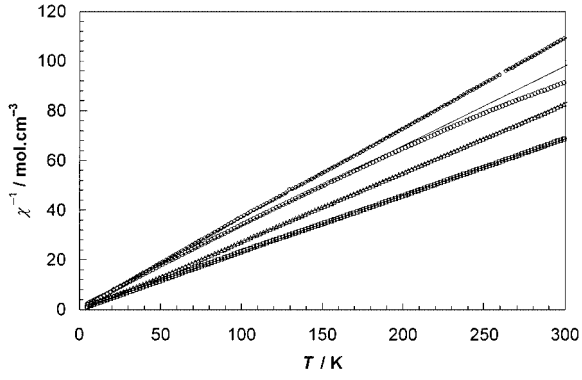

Figure 3. Temperature dependence of reciprocal susceptibility for **1** (diamonds), **2** (squares), **3** (triangles) and **4** (circles). Solid lines represent best fits to Curie–Weiss law.

The room temperature magnetic moments of the complexes **1** (4.7 μ_B), **2** (5.9 μ_B), **3** (5.4 μ_B) and **4** (5.1 μ_B) are

indicative of maximum spin multiplicity for all four compounds. The observed magnetic moments for **1**, **3** and **4** deviate noticeably from the spin only values [4.90 μ_B for S = 2 (Cr and Fe) or 3.87 μ_B for S = 3/2 (Co)], but are well within the ranges usually observed for high-spin d^4, d^6 and d^7 metals.[77]

The high spin (S = 2) ground state of planar bis(amidinate) **3** contrasts with the more usual observation of an intermediate spin state (S = 1) for Fe^{II} complexes with this geometry,[60,61] and is more common for tetrahedral Fe^{II}.[37,78] The planar Fe^{II} complexes of N_4 macrocycles and dithiolates all exhibit intermediate spin states,[64,66–75] with the planar, but high-spin, salen[62] and calix[4]arene[63] complexes of Fe^{II} constituting the only exceptions.

^{1}H NMR Spectroscopy

The room-temperature ^{1}H NMR spectrum of the diamagnetic Ni complex **5** in [D_6]benzene shows two septuplets for the isopropyl methine protons and four doublets for the isopropyl methyl protons. This is consistent with the approximate D_2 symmetry observed in the solid state in which the aromatic rings are tilted with respect to the N_4Ni coordination plane. This inclination establishes a propeller-like arrangement of the six aromatic rings, thus imparting a screw-sense to the molecule. Apparently, libration of the aryl groups, inverting the screw sense through a D_{2h}-symmetric transition state (Figure 4), is slow on the NMR time scale at ambient temperature. Warming a solution of **5** in [D_8]toluene results in gradual broadening of the isopropyl resonances, but coalescence is not yet reached at 110 °C. Nevertheless, slow chemical exchange of the two isopropyl methine and the two sets of methyl signals is confirmed by positive cross-peaks in the EXSY 2D-spectrum.

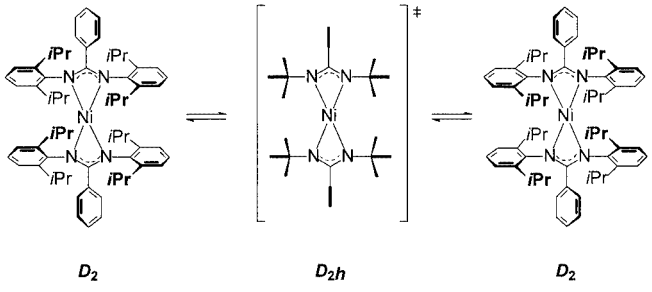

Figure 4. Epimerisation process in [{PhC(NAr)$_2$}$_2$Ni] (**5**).

The rate constant for the interconversion of the enantiomers k = 2.25(38) s^{-1} at 338 K was obtained by plotting the extent of exchange vs. the mixing time.[79] The free energy of activation $\Delta G^{\ddagger}_{338}$ = 80.9(4) kJ·mol^{-1} was calculated from the rate constant k.[80]

In contrast to the Ni complex, the paramagnetic bis(amidinates) **1**–**4** exhibit broad, shifted lines in their ^{1}H NMR spectra in [D_6]benzene. The Cr complex **1** shows resonances in the region +20 to –10 ppm. Severe overlap of the resonances renders the spectrum uninformative. The resonances of the Mn derivative **2** appear in the same spectral region, with even more line-broadening and inherent overlap of resonances. In contrast, the Fe and Co bis(amidinate) complexes display spectra that consist mainly of well-separated, broad singlets. The chemical shifts in the ^{1}H NMR spectrum of the Fe complex **3** span a range from ca. +60 to –30 ppm, displaying 11 lines. For the Co complex **4**, twelve lines are observed from ca. +120 ppm to –140 ppm. Full interpretation of these spectra is complicated, but the number of resonances indicates that the solution structures have symmetries lower than D_{2h} (**3**) and D_{2d} (**4**). This strongly suggests that also for the Fe and the Co derivatives the sterically demanding aryl substituents cause restricted motion of the aryl rings in solution.

Calculations

DFT calculations were used to obtain more insight into the factors that determine the coordination geometry of these complexes. In order to separate electronic from steric contributions, calculations were performed on the model complexes [{HC(NH)$_2$}$_2$M] containing an unsubstituted formamidinate ligand. The system was studied at the B3LYP/SV level using the GAMESS-UK program,[81] using the spin-restricted (S = 0) or spin-unrestricted ($S > 0$) formalism; see Exp. Sect. for details. For every metal, both planar and perpendicular geometries were optimised (constrained to D_{2h} and D_{2d} symmetry, respectively); the spin states assumed for these calculations were the ones found experimentally for the fully substituted system. In Table 2, the geometries calculated to be most stable for the model system are compared to those observed experimentally. The energy differences between the calculated perpendicular and planar geometries are included.

Table 2. Relative energies of tetrahedral vs. planar geometries of [{HC(NH)$_2$}$_2$M] by DFT calculations.

	X-ray [{PhC(NAr)$_2$}$_2$M]	S	B3LYP/SV [{HC(NH)$_2$}$_2$M]	$\Delta E_{\text{tet.–pla}n}$ [kJ·mol^{-1}]
Cr	planar	2	planar	100
Mn	tetrahedral	5/2	tetrahedral	–27.3
Fe	planar	2	tetrahedral	–10.1
Co	tetrahedral	3/2	tetrahedral	–23.2
Ni	planar	0	planar	–[a]

[a] No reasonable orbital occupation for perpendicular S = 0 structure.

For the model complexes, most of the geometries predicted on electronic grounds match the experimental ones, except for Fe (Table 2). However, the calculated energy difference between the two geometries is significantly smaller for Fe than for either Mn or Co. These results for the model system indicate that the observed geometries are determined mainly by the intrinsic electronic preference of the metal. For the special case of Fe, where this preference is calculated to be small, steric factors probably dominate; these seem to favour the planar structure due to a more efficient reduction of interligand repulsion by tilting of the aryl substituents.

Decrease of Ligand Size

To see whether a slight decrease in ligand steric demand could already cause a reversion of the Fe^{II} bis(amidinate) structure to distorted tetrahedral, the asymmetric amidinate ligand $[PhC(NAr)(NXyl)]^-$ (Ar = 2,6-$iPr_2C_6H_3$, Xyl = 2,6-$Me_2C_6H_3$) was prepared. Reaction of $FeCl_2$ with 2 equiv. of the amidinate lithium salt resulted in formation of *cis*-$[\{PhC(NAr)(NXyl)\}_2Fe]$ (**6**, Scheme 2) that was characterised by single-crystal X-ray diffraction.

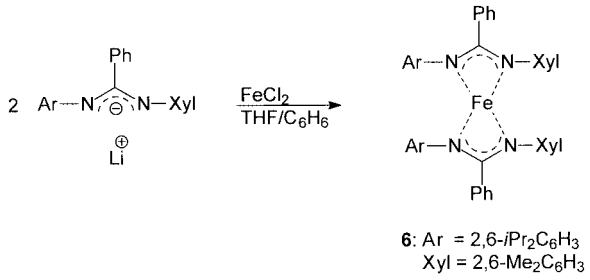

6: Ar = 2,6-$iPr_2C_6H_3$
Xyl = 2,6-$Me_2C_6H_3$

Scheme 2.

The molecular structure of **6** is shown in Figure 5 and selected bond angles and bond lengths are listed in Table 3. It is seen that even with this smaller, asymmetric ligand, the complex still adopts a distorted square-planar geometry. Remarkably, the two 2,6-$iPr_2C_6H_3$ groups are located on the same side of the molecule, with their *i*Pr substituents interlocking in a similar fashion as observed in complex **3**. The NFeN coordination planes in **6** are inclined at an angle of 14.21(6)°, which is only about 2° larger than in **3**. The room-temperature magnetic moment of **6** is 5.6 μ_B, indicative of high-spin Fe^{II}. Despite the difference in steric demand of the substituents, the two Fe–N distances in **6** are essentially equal, but the interligand N–Fe–N angle is noticeably larger on the side with the Ar substituents [125.51(4)°] than on the side with the Xyl substituents [105.97(4)°]. As is the case in the other complexes, the NAr nitrogen atom deviates slightly from planarity ($\Sigma_{\angle N1}$ = 354.64°), whereas the NXyl nitrogen atom is close to perfectly planar ($\Sigma_{\angle N2}$ = 359.03°).

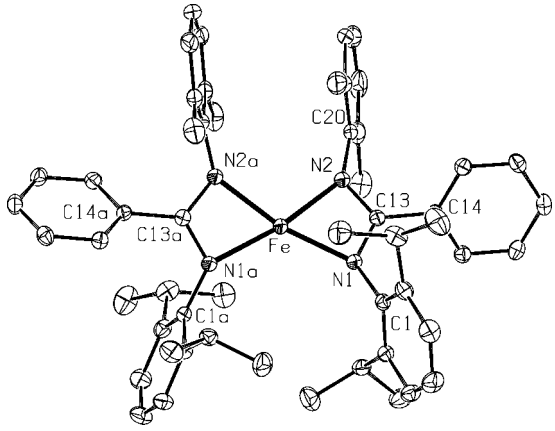

Figure 5. Molecular structure of [{PhC(NAr)(NXyl)}Fe] (**6**) (50% ellipsoids). Hydrogen atoms and cocrystallised benzene molecule have been omitted for clarity.

Table 3. Selected interatomic distances and angles for $[\{Ph(NAr)(NXyl)\}_2Fe]$ (**6**).

Distances [Å]			
Fe–N1	2.0639(10)	N1–C13	1.3408(14)
Fe–N2	2.0697(10)	N2–C13	1.3280(14)
Angles [°]			
N1–Fe–N2	64.82(4)	Fe–N2–C13	91.51(7)
N1–Fe–N1_a	125.51(4)	Fe–N2–C20	140.27(8)
N2–Fe–N2_a	105.97(4)	C13–N2–C20	127.25(10)
N1–Fe–N2_a	167.58(4)	N1–C13–N2	112.23(10)
Fe–N1–C1	140.02(8)	N1–C13–C14	123.71(10)
Fe–N1–C13	91.40(7)	N2–C13–C14	124.06(10)
C1–N1–C13	123.22(9)		

Conclusions

The coordination geometry of the bis(amidinate) complexes of the divalent first-row transition metal ions is governed by a subtle balance between electronic and steric factors. This balance can be tipped by variation of the substituents on the amidinate nitrogen atoms. It was shown by Winter et al. that substituents with steric demand in the amidinate plane (*t*Bu) can force an ion with an electronic preference for a planar geometry (Cr^{II}) to adopt a tetrahedral structure.[36] The work presented here shows that substituents with steric demand above and below the amidinate plane (2,6-$iPr_2C_6H_3$) can force an ion with a mild preference for a tetrahedral geometry (Fe^{II}) to adopt a planar one. Apparently, in this geometry the interligand steric interactions can be more effectively diminished by tilting the aryl rings to allow interlocking of the *i*Pr substituents.

These substituted amidinate ligands provide a simple way to generate rare high-spin (S = 2) Fe^{II} complexes with a planar geometry. It should be interesting to study the reactivity of these species (especially towards oxygen transfer agents) and compare that with the more extensively studied reactivity of planar intermediate spin (S = 1) Fe^{II} systems such as porphyrin and phthalocyanin complexes.

Experimental Section

General Remarks: All manipulations involving air-sensitive compounds were carried out under nitrogen using standard Schlenk and drybox techniques. Diethyl ether and THF (99.9% Aldrich) were percolated through a column of Al_2O_3 and stored under nitrogen. Toluene, hexane and pentane (99.9% Aldrich) were percolated through a column packed with molecular sieves (4 Å) (90 wt-%) and Al_2O_3 (10 wt-%) and stored under nitrogen. Benzene was distilled from Na/K alloy. Deuterated solvents (Aldrich) were dried with Na/K alloy and vacuum-transferred before use. Magnetic susceptibility measurements were performed with a Quantum Design MPMS-7 SQuID magnetometer of the department of Solid State Chemistry at the University of Groningen. NMR spectra were recorded with Varian Inova 500, VXR 300 and Gemini 200 instruments. IR spectra were recorded with a Mattson 4020 Galaxy FT–IR spectrometer. Elemental analyses were performed by the Microanalytical Department at the University of Groningen or by Mikroanalytisches Laboratorium H. Kolbe, Mülheim an der Ruhr,

Germany. Anhydrous $FeCl_2$[82] and $CoCl_2$[83] and [(DME)$NiBr_2$][84] were prepared according to published procedures. All other chemicals were commercially available products, which were used without further purification.

***N*-(2,6-Diisopropylphenyl)benzanilide:** Benzoyl chloride (39 mL, 0.33 mol) was added to a vigorously stirred mixture of 10% aqueous NaOH (240 mL) and 2,6-diisopropylaniline (57.0 mL, 0.30 mol). After 60 min, the solid was collected on a glass filter and washed several times with water, and once with ethanol. The product was dried in vacuo and isolated as a white powder. Yield: 57.6 g (0.19 mol, 65%). ^{1}H NMR (200 MHz, [D_1]chloroform, room temp.): δ = 7.92 (d, J = 6.6 Hz, 2 H, ArH), 7.58–7.05 (m, 8 H, ArH), 3.15 (sept, J = 6.8 Hz, 2 H, *i*Pr-CH), 1.22 (d, J = 6.8 Hz, 6 H, *i*Pr-CH_3) ppm. IR (KBr): $\tilde{\nu}$ = 3302 cm^{-1} (m), 3293 (m), 3270 (m), 2956 (m), 2923 (s), 2854 (m), 1640 (s), 1580 (w), 1515 (m), 1486 (m), 1463 (m), 1453 (m), 1380 (w), 1361 (w), 1291 (w) cm^{-1}.

***N*-(2,6-Diisopropylphenyl)benzimidoyl Chloride:** A mixture of *N*-(2,6-diisopropylphenyl)benzanilide (57.6 g, 0.19 mol) and thionyl chloride (43.1 mL, 0.58 mol) was refluxed for 1 h. The remainder was distilled using a Kugelrohr apparatus (oven 200 °C, 0.02 Torr), to give the imidoyl chloride as a yellow, slowly solidifying oil. Yield: 51.3 g (0.17 mol, 90%). ^{1}H NMR (300 MHz, [D_1]chloroform, room temp.): δ = 8.26 (d, J = 5.2 Hz, 2 H, ArH), 7.61–7.50 (m, 3 H, ArH), 7.24 (s, 3 H, ArH), 2.88 (sept, J = 4.4 Hz, 2 H, *i*Pr-CH), 1.27 (d, J = 4.4 Hz, 6 H, *i*Pr-CH_3), 1.21 (d, J = 4.4 Hz, 6 H, *i*Pr-CH_3) ppm. IR (KBr): $\tilde{\nu}$ = 2959 (s), 2926 (s), 1665 (s), 1582 (w), 1462 (m), 1451 (m), 1167 (m), 398 (m), 797 (w), 760 (m), 986 (m) cm^{-1}.

***N*,*N*′-Bis(2,6-diisopropylphenyl)benzamidine and *N*-(2,6-Diisopropylphenyl)-*N*′-(2,6-dimethylphenyl)benzamidine:** The amidines were prepared from *N*-(2,6-diisopropylphenyl)benzimidoyl chloride and the appropriate aniline according to a previously reported procedure.[9] Yield and characterisation data for *N*,*N*′-bis(2,6-diisopropylphenyl)benzamidine have been published.[9] Data for *N*-(2,6-diisopropylphenyl)-*N*′-(2,6-dimethylphenyl)benzamidine (obtained as a mixture of isomers): Yield: 7.4 g (19 mmol, 84%). ^{1}H NMR (300 MHz, [D_1]chloroform, room temp.): δ = 7.53–6.70 (m, 11 H, ArH), 5.78, 5.75 (2× s overlapping, 1 H, NH), 3.62–3.11 (4× sept overlapping, 2 H, *i*Pr-CH), 2.42, 2.17, 2.10 (3× s overlapping, 6 H, Xyl-CH_3), 1.42, 1.30, 1.07, 0.97 (4× d, J = 6.6 Hz, 12 H, *i*Pr-CH_3) ppm. ^{13}C NMR (75 MHz, [D_1]chloroform, room temp.): δ = 154.0, 153.5 (N*C*N), 145.8, 144.9, 143.4, 139.2, 137.1, 135.4, 134.6, 134.4, 134.0 (ArC_{ipso}), 129.3, 129.2 (Ar*C*H), 128.8 (ArC_{ipso}), 128.6, 128.4, 128.0, 127.6, 127.5, 126.9, 126.3, 123.5, 123.3, 122.9 (Ar*C*H), 28.4, 28.1 (*i*Pr-*C*H), 24.4, 24.3, 22.8, 21.9 (*i*Pr-*C*H_3), 18.9, 17.6 (Xyl-*C*H_3) ppm. IR (KBr): $\tilde{\nu}$ = 3424 (w, NH), 3354 (m, NH), 3058 (m), 2942 (s), 2915 (s), 1642 (s), 1614 (s), 1588 (s), 1574 (s), 1494 (m), 1435 (s), 1355 (s), 1326 (m), 1301 (w), 1273 (w), 1255 (w), 1220 (w), 1192 (m), 1179 (m), 1162 (w), 1109 (w), 1099 (w), 1077 (w), 1060 (w), 1043 (w), 1026 (w), 923 (w), 898 (w), 835 (w), 806 (w), 775 (s), 742 (w), 697 (s), 616 (w), 600 (w), 577 (w), 543 (w), 516 (w), 507 (w), 487 (w) cm^{-1}. HRMS (EI): calcd. for $C_{27}H_{32}N_2$: 384.2565; found: 384.2571.

Complexes [{PhC(NAr)$_2$}$_2$M] (1–5). General Procedure: [PhC(NAr)$_2$]H (1.0 g, 2.3 mmol) was dissolved in THF (10 mL). *n*BuLi (2.5 M in hexanes, 0.91 mL, 2.3 mmol) was added and the solution was stirred for 30 min. The solution of Li[PhC(NAr)$_2$] thus obtained was added dropwise to a suspension of MCl_2 (1.1 mmol) in THF (10 mL). The mixture was stirred under the conditions mentioned below for the various derivatives. After the reaction, the solvent was pumped off and the residue was freed of any residual THF by suspending it in pentane (10 mL) and subsequent removal of all volatiles in vacuo. The residue was repeatedly extracted with pentane (10 mL, unless mentioned otherwise) until the extracts were colourless. The extract was concentrated and cooled to afford the crystalline bis(amidinate) complex, which was isolated by filtration and dried in vacuo.

[{PhC(NAr)$_2$}$_2$Cr] (1): The general procedure was applied using 0.76 g [PhC(NAr)$_2$]H (1.7 mmol) and 0.11 g $CrCl_2$ (0.86 mmol). The reaction was stirred for 15 h at room temperature. Extraction and crystallisation were carried out using hexanes. The product was obtained as red crystals. Yield: 0.48 g (0.52 mmol, 61%). ^{1}H NMR (300 MHz, [D_6]benzene, room temp.) by deconvolution: δ ($\Delta\nu_{1/2}$) = 15.3 (194), 14.4 (239), 7.0 (140), 5.0 (939), 2.5 (250), 0.9 (5396), –7.6 (205) ppm (Hz); integral ratio 2:2:2:23:1:20:1. $C_{62}H_{78}CrN_4$ (931.32): calcd. C 79.96, H 8.44, N 6.02; found C 79.31, H 8.49, N 5.95.

[{PhC(NAr)$_2$}$_2$Mn] (2): The general procedure was applied for ligand deprotonation using 1.0 g amidine (2.3 mmol). $MnCl_2$ (143 mg, 1.1 mmol) was added as a solid to the Li[PhC(NAr)$_2$] solution. The reaction mixture was stirred for 2 h at room temperature, during which no significant colour change was observed. Off-white crystals were obtained from pentane at –25 °C. Yield: 0.51 g (0.54 mmol, 48%). ^{1}H NMR (300 MHz, [D_6]benzene, room temp.) by deconvolution: δ ($\Delta\nu_{1/2}$) = 15.1 (2761), 14.1 (566), 6.2 (1465), 3.5 (230), –4.2 (784) ppm (Hz); integral ratio 1:2:11:1:6. $C_{62}H_{78}MnN_4$ (934.27): calcd. C 79.71, H 8.42, N 6.00; found C 79.97, H 8.48, N 5.89.

[{PhC(NAr)$_2$}$_2$Fe] (3): The general procedure was applied. The reaction mixture was stirred for 2 h at room temperature, during which the solution turned dark green. Extraction was performed with hexanes. The product was isolated as dark green crystals after recrystallisation from hexanes. Yield: 0.98 g (1.0 mmol, 91%). ^{1}H NMR (300 MHz, [D_6]benzene, room temp.): δ = ($\Delta\nu_{1/2}$, integral) = 57.4 (952, 4 H), 31.9 (74.6, 4 H), 22.2 (74.5, 4 H), 16.8 (61.0, 4 H), 14.8 (158, 12 H), 6.23 (140, 4 H), 3.80 (126, 12 H), –2.05 (54.5, 2 H), –5.19 (89.7, 12 H), –6.18 (64.5, 4 H), –29.2 (274, 12 H) ppm (Hz); one of two expected *i*Pr-CH resonances not observed, possibly due to extreme line-broadening. $C_{62}H_{78}FeN_4$ (935.18): calcd. C 79.63, H 8.41, N 5.99; found C 79.44, H 8.47, N 6.05.

[{PhC(NAr)$_2$}$_2$Co] (4): The general procedure was applied, but in this case no colour change was observed after stirring at room temperature for 30 min. Upon warming the suspension at 50 °C for 30 min, a colour change from green to dark red was observed. The Co complex was obtained as red crystals after recrystallisation of the crude product from hexanes. Yield: 0.70 g (0.74 mmol, 65%). ^{1}H NMR (500 MHz, [D_6]benzene, room temp.): δ ($\Delta\nu_{1/2}$, integral) = 115 (697), 60.9 (140, 4 H), 45.3 (1994), 35.0 (80.9, 2 H), 24.8 (110, 12 H), 21.2 (129, 4 H), 2.77 (119, 4 H), –19.0 (86.6, 4 H), –69.6 (1007), –73.2 (431, 12 H), –84.0 (85.8, 12 H), –138 (2461) ppm (Hz); integration of resonances at δ = 115, 45.3, –69.6 and –138 ppm inaccurate due to extreme broadness. $C_{62}H_{78}CoN_4$ (938.26): calcd. C 79.37, H 8.38, N 5.97; found C 78.60, H 8.42, N 5.88.

[{PhC(NAr)$_2$}$_2$Ni] (5): The general procedure was applied using 0.53 g (1.2 mmol) [PhC(NAr)$_2$]H and [(DME)$NiBr_2$] (0.19 g, 0.6 mmol) as Ni source. The reaction mixture was stirred under reflux conditions for 66 h. The crude product was recrystallised from toluene and the resulting red crystals were washed with diethyl ether. Yield: 0.26 g (0.30 mmol, 47%). ^{1}H NMR (300 MHz, [D_6]benzene, room temp.): δ = 6.87–7.03 (m, 12 H), 6.41–6.64 (m, 10 H), 4.24 (sept, J = 7.0 Hz, 4 H), 3.13 (sept, J = 7.0 Hz, 4 H), 2.31 (d, J = 7.0 Hz, 12 H), 1.55 (d, J = 7.0 Hz, 12 H), 0.60 (d, J = 7.0 Hz, 12 H), 0.49 (d, J = 7.0 Hz, 12 H) ppm. ^{13}C NMR (75 MHz, [D_6]benzene, room temp.): δ = 175.1 (NCN), 144.5, 143.3, 141.5

(3 × *ipso*-C), 130.8, 130.4 (*ipso*-C), 129.6, 126.8, 125.7, 124.9, 123.6, 29.4, 28.5 (2 × *i*Pr-CH), 24.4, 24.0, 22.3, 21.4 (4 × *i*Pr-CH_3) ppm. $C_{62}H_{78}N_4Ni$ (938.04): calcd. C 79.38, H 8.38, N 5.97; found C 79.37, H 8.29, N 5.88.

[{PhC(NAr)(NXyl)}$_2$Fe] (6): $LiCH_2SiMe_3$ (0.13 g, 1.4 mmol) was added to a stirred solution of *N*-(2,6-diisopropylphenyl)-*N*′-(2,6-dimethylphenyl)benzamidine (0.53 g, 1.4 mmol) in 15 mL 1% THF/C_6H_6 at room temperature. After 15 min, $FeCl_2$ (0.09 g, 0.7 mmol) was added to the yellow solution. The colour of the mixture changed from yellow to green. The reaction mixture was stirred for 2 h after which the solvents were removed in vacuo. Residual THF was removed by suspending the residue in pentane that was subsequently pumped off. The solid was extracted with benzene (40 mL) until the extracts were colourless. The crude product was recrystallised from hot benzene, affording **6**·C_6H_6 as green crystals. Yield: 0.32 mg (0.4 mmol, 50%).^{1}H NMR (300 MHz, [D_6]benzene, room temp.): δ = ($\Delta\nu_{1/2}$, integral): 26.07 (25, 4 H), 25.15 (25, 4 H), 16.55 (18, 4 H), 11.79 (235, 12 H), 4.02 (74, 4 H), 0.46 (43, 12 H), –2.57 (19, 2 H), –5.48 (183, 12 H), –7.24 (22, 2 H), –9.24 (22, 2 H) ppm (Hz). $C_{54}H_{62}FeN_4$·C_6H_6 (901.07): calcd. C 80.0, H 7.6, N 6.2; found C 79.6, H 7.8, N 6.3.

Determination of *k* and $\Delta G^{\ddagger}$ for Epimerisation of 5: ^{1}H 2D EXSY spectra (500 MHz, [D_8]toluene, 338 K) were obtained using the NOESY sequence (d_1–90°–d_2–90°–τ–90°–FID) with an extra gradient during the mixing time τ. The spectral width was 8000 Hz. Mixing times of 0.2, 0.3, 0.4 and 0.5 s were used. The relaxation delay d_1 was 1 s and the increment for the evolution time d_2 was 98 μs. Peak volumes of the isopropyl methine resonances (δ = 4.24 and 3.13 ppm) and their cross-peaks were determined by means of the Gaussian method in the integration program Sparky.[85] The ratio of the peak volumes of the cross-peaks and the diagonal peaks (I_x/I_d) was plotted vs. mixing time τ. The rate constants k for the exchange process was determined by fitting the data to the equation[79]

$$\frac{I_x}{I_d} = \frac{1 - e^{-2k\tau}}{1 + e^{-2k\tau}}$$

The free energy of activation $\Delta G^{\ddagger}$ at 338 K was calculated by substitution of k_{338} according to the relation[80]

$$k = \frac{\kappa k_b T}{h} \cdot e^{-\Delta G^{\ddagger}/RT}$$

Magnetic Measurements: Data were collected on crystalline samples (ca. 25 mg) from 300 to 5 K at a field of 1000 G. Measured magnetic susceptibilities are corrected for diamagnetism using Pascal's constants.[86] Effective magnetic moments are calculated as

$$\mu_{eff.} = 2.828\sqrt{\chi_m T}$$

X-ray Crystallographic Study: Single crystals suitable for X-ray diffraction were obtained by recrystallisation from pentane (**1**), hexanes (**2**, **3**), benzene (**4**, **6**) or diethyl ether (**5**). Some crystals were found to contain cocrystallised solvent molecules (**2**·*n*-hexane, **4**·2C_6H_6 and **6**.C_6H_6). The crystals were mounted on top of a glass fibre, by using inert-atmosphere handling techniques, and aligned on a Bruker[87] SMART APEX CCD diffractometer (Platform with full three-circle goniometer). The diffractometer was equipped with a 4 K CCD detector set 60.0 mm from the crystal. The crystals were cooled using the Bruker KRYOFLEX low-temperature device. Intensity measurements were performed using graphite-monochromated Mo-K_α radiation from a sealed ceramic diffraction tube (SIEMENS). Generator settings were 50 kV/40 mA. SMART[87] was used for preliminary determination of the unit cell constants and data collection control. The intensities of reflections of a hemisphere were collected by a combination of 3 sets of exposures (frames). Each set had a different φ angle for the crystal and each exposure covered a range of 0.3° in ω. A total of 1800 frames were collected with an exposure time of 20.0 s (**1**, **2**, **5**) or 10.0 s (**3**, **4**, **6**) per frame. Data integration and global cell refinement was performed with the program SAINT.[87] The final unit cell was obtained from the *xyz* centroids of 5709 (**1**), 3348 (**2**), 6534 (**3**), 4586 (**4**), 5447 (**5**), 9843 (**6**) reflections after integration. Intensity data were corrected for Lorentz and polarisation effects, scale variation, for decay and absorption: a multi-scan absorption correction was applied, based on the intensities of symmetry-related reflections measured at different angular settings (SADABS),[88] and reduced to F_o^2. The program suite SHELXTL was used for space group determination (XPREP).[87] The unit cells[89] were identified as monoclinic; reduced cell calculations did not indicate any higher metric lattice symmetry.[90] For **4**, The |*E*| distribution statistics were ambiguous about a centrosymmetric/non-centrosymmetric space group.[91] The space groups were derived from the systematic extinctions. Examination of the final atomic coordinates of the structure did not yield extra symmetry elements.[92] The structures of **1**, **2**, **4**, **5** and **6** were solved by Patterson methods and extension of the model was accomplished by direct methods applied to difference structure factors using the program DIRDIF.[93] For **3**, the structure was solved by direct methods with SIR-97.[94,95] The positional and anisotropic displacement parameters for the non-hydrogen atoms were refined. The unit cell of **2** contains a molecule of hexane solvent of which one end is highly disordered. One of the C atoms (C68) was described as occupying two positions with separately refined site occupancy factors. The s.o.f. of the major fraction refined to a value of 0.625(13). Refinement for **4** was complicated by a twinning problem. After introducing a twin matrix as detected by PLATON ([–1 0 0 0 –1 0 0.99 0 1], 180° rotation about the *c** axis), with scale factors for the fractional contributions of the various twin components, the structure refined smoothly. The s.o.f. of the major fraction of the component of the twin model refined to a value of 0.629(3). All hydrogen atoms of **1**, **2**, **5** and **6** (except those belonging to the disordered hexane solvent molecule in **2**) were located from a subsequent difference Fourier synthesis, and their coordinates and isotropic displacement parameters were refined. For **3**, Fourier synthesis resulted in the location of most of the hydrogen atoms. The remaining hydrogen atoms in **3** and all hydrogen atoms in **4** were included in the final refinement riding on their carrier atoms with their positions calculated by using sp^2 or sp^3 hybridisation at the C atom as appropriate with U_{iso} = c × U_{equiv} of their parent atom, where c = 1.2 for the non-methyl hydrogen atoms and c = 1.5 for the methyl hydrogen atoms and where values U_{equiv} are related to the atoms to which the H atoms are bonded. The methyl groups were refined as rigid groups, which were allowed to rotate freely. Neutral atom scattering factors and anomalous dispersion corrections were taken from International Tables for Crystallography.[96] All refinement calculations and graphics were performed with the program packages SHELXL[97] (least-square refinements) and PLATON[98,99] (calculation of geometric data and ORTEP illustrations). No classic hydrogen bonds, no missed symmetry (MISSYM), but potential solvent-accessible

area [voids of 325.2 (**1**), 78.7 (**2**), 372.6 (**3**), 111.2 (**4**) and 296.4 (**5**) Å^3/unit cell] were detected by procedures implemented in PLATON.[98,99] Crystallographic data for **1**–**6** and details of the refinement are listed in Table 4 and Table 5. CCDC-247623 to -247628 contain the supplementary crystallographic data for this paper. These data can be obtained free of charge from The Cambridge Crystallographic Data Centre via www.ccdc.cam.ac.uk/data_request/cif.

Table 4. Crystal, collection and refinement data for complexes **1**–**3**.

	1	**2**	**3**
Empirical formula	$C_{62}H_{78}N_4Cr$	$C_{62}H_{78}MnN_4{\cdot}C_6H_{14}$	$C_{62}H_{78}FeN_4$
Formula mass	931.32	1020.44	935.18
Crystal dimensions [mm]	0.37 × 0.13 × 0.034	0.22 × 0.16 × 0.14	0.40 × 0.40 × 0.08
Colour, habit	red, platelet	pale yellow, block	green, platelet
Crystal system	monoclinic	monoclinic	monoclinic
Space group (no.)[96]	$P2_1/c$ (#14)	$P2_1/c$ (#14)	$P2_1/c$ (#14)
a [Å]	23.795(1)	11.9048(5)	23.846(1)
b [Å]	10.3509(4)	24.826(1)	10.3346(6)
c [Å]	25.189(1)	20.7161(8)	25.211(1)
β [°]	115.714(1)	96.035(1)	115.898(1)
Z	4	4	4
V [Å^3]	5589.7(4)	6088.7(4)	5589.0(5)
$\rho_{calcd.}$ [g/cm^3]	1.107	1.113	1.111
θ range [°]	2.18–26.37	2.14–26.37	2.37–29.80
λ [Å]	0.71073 (Mo-K_α)	0.71073 (Mo-K_α)	0.71073 (Mo-K_α)
T [K]	100(1)	110(1)	105(1)
Data collect. time [h]	13.0	13.6	8.9
No. of measured reflections	43872	48623	43919
No. of unique reflections	11424	12423	14931
μ [cm^{-1}]	2.45	2.59	3.1
No. of parameters	916	983	913
Weighting scheme a, b[a]	0.0559, 0.7843	0.0797, 0.0	0.0842, 1.6145
$R(F)$ for $F_o \geq 4\sigma(F_o)$[b]	0.0483	0.0642	0.0519
$wR(F^2)$[c]	0.1213	0.1719	0.1454
Residual electron density [e Å^{-3}]	–0.27, 0.33(6)	–0.44, 0.56(6)	–0.38, 2.38(7)
GoF[d]	1.017	0.993	1.024

[a] $w = 1/[\sigma^2(F_o^2) + (aP)^2 + bP]$, $P = [\max(F_o^2,0) + 2F_c^2]/3$. [b] $R(F) = \Sigma(||F_o| - |F_c||)/|F_o|$. [c] $wR(F^2) = \{\Sigma[w(F_o^2 - F_c^2)^2]/\Sigma[w(F_o^2)^2]\}^{1/2}$. [d] GoF = $\{\Sigma[w(F_o^2 - F_c^2)^2]/(n - p)\}^{1/2}$, n = # refl., p = # param. refined.

Table 5. Crystal, collection and refinement data for complexes **4**–**6**.

	4	**5**	**6**
Empirical formula	$C_{62}H_{78}CoN_4{\cdot}2C_6H_6$	$C_{62}H_{78}N_4Ni$	$C_{54}H_{62}FeN_4{\cdot}C_6H_6$
Formula mass	1049.49	938.02	901.08
Crystal dimensions [mm]	0.24 × 0.19 × 0.12	0.19 × 0.13 × 0.07	0.55 × 0.42 × 0.21
Colour, habit	red/brown, block	red, block	green, block
Crystal system	monoclinic	monoclinic	monoclinic
Space group (no.)[96]	$P2_1/c$ (#14)	$C2/c$ (#15)	$C2/c$ (#15)
a [Å]	18.028(5)	23.052(2)	8.9541(3)
b [Å]	18.145(5)	10.6550(8)	24.3880(9)
c [Å]	20.797(6)	24.402(2)	23.5938(9)
β [°]	113.146(5)	113.667(1)	99.936(1)
Z	4	4	4
V [Å^3]	6255(3)	5489.5(8)	5075.0(3)
$\rho_{calcd.}$ [g/cm^3]	1.162	1.135	1.179
θ range [°]	2.22–22.21	2.47–28.60	2.42–28.28
λ [Å]	0.71073 (Mo-K_α)	0.71073 (Mo-K_α)	0.71073 (Mo-K_α)
T [K]	110(2)	100(1)	100(1)
Data collect. time [h]	8.0	13.0	8.0
No. of measured reflections	53509	21358	23145
No. of unique reflections	7864	5575	6269
μ [cm^{-1}]	3.19	3.94	3.39
No. of parameters	730	459	430
Weighting scheme a, b[a]	0.0016, 46.8803	0.0304, 5.30	0.0565, 1.690
$R(F)$ for $F_o \geq 4\sigma(F_o)$[b]	0.0938	0.0490	0.0359
$wR(F^2)$[c]	0.2390	0.1041	0.0973
Residual electron density [e/Å^{-3}]	–0.19, 0.24(4)	–0.24, 0.43(6)	–0.25, 0.41(5)
GoF[d]	0.957	1.005	1.083

[a] $w = 1/[\sigma^2(F_o^2) + (aP)^2 + bP]$, $P = [\max(F_o^2,0) + 2F_c^2]/3$. [b] $R(F) = \Sigma(||F_o| - |F_c||)/\Sigma|F_o|$. [c] $wR(F^2) = \{\Sigma[w(F_o^2 - F_c^2)^2]/\Sigma[w(F_o^2)^2]\}^{1/2}$. [d] GoF = $\{\Sigma[w(F_o^2 - F_c^2)^2]/(n - p)\}^{1/2}$, n = # refl., p = # param. refined.

DFT Calculations: All calculations on the model complexes [{HC(NH)$_2$}$_2$M] were carried out with the GAMESS-UK program.[81] Geometries were optimised at the B3LYP level[100–102] within either D_{2h} or D_{2d} symmetry using the 3-21G basis set[103] on the ligand atoms and LANL2DZ (small-core pseudopotential) on the metal atom.[104–106] Calculations used the spin-restricted (for $S = 0$ states) or spin-unrestricted (for $S > 0$ states) formalism; in the latter case, spin contamination was uniformly found to be negligible.

Supporting Information (see also footnote on the first page of this article): IR data for complexes **1**–**6** and total energies and S^2 values for all calculations mentioned in the text (Table S.1).

Acknowledgments

We thank J. Baas for performing the magnetic susceptibility measurements.

Note Added in Proof (April 15, 2005): A recent paper describes a planar bis(amidinate)magnesium complex with ligands related to those used in this paper: R. T. Boeré, M. L. Cole, P. C. Junk, *New J. Chem.* **2005**, *29*, 128–134.

[1] F. T. Edelmann, *Coord. Chem. Rev.* **1994**, *137*, 403–481.
[2] J. Barker, M. Kilner, *Coord. Chem. Rev.* **1994**, *133*, 219–300.
[3] E. A. C. Brussee, A. Meetsma, B. Hessen, J. H. Teuben, *Chem. Commun.* **2000**, 497–498.
[4] E. A. C. Brussee, A. Meetsma, B. Hessen, J. H. Teuben, *Organometallics* **1998**, *17*, 4090–4095.
[5] C. Averbuj, E. Tish, MS Eisen, *J. Am. Chem. Soc.* **1998**, *120*, 8640–8646.
[6] V. Volkis, M. Shmulinson, C. Averbuj, A. Lisovskii, F. T. Edelmann, MS Eisen, *Organometallics* **1998**, *17*, 3155–3157.
[7] T. Boussie, V. Murphy, J. A. Van Beek, WO 99/05154 to SYMYX Technologies, **1999**.
[8] K. Yokota, US6107232 to Idemitsu Kosan Co., Ltd., **2000**.
[9] S. Bambirra, D. van Leusen, A. Meetsma, J. H. Teuben, *Chem. Commun.* **2003**, 522–523.
[10] M. J. R. Brandsma, E. A. C. Brussee, A. Meetsma, B. Hessen, J. H. Teuben, *Eur. J. Inorg. Chem.* **1998**, 1867–1870.
[11] M. P. Coles, R. F. Jordan, *J. Am. Chem. Soc.* **1997**, *119*, 8125–8126.
[12] J. M. Decker, S. J. Geib, T. Y. Meyer, *Organometallics* **1999**, *18*, 4417–4420.
[13] J. C. Flores, J. C. W. Chien, M. D. Rausch, *Organometallics* **1995**, *14*, 1827–1833.
[14] D. Herskovics-Korine, MS Eisen, *J. Organomet. Chem.* **1995**, *503*, 307–314.
[15] R. J. Keaton, K. C. Jayaratne, D. A. Henningsen, L. A. Koterwas, L. R. Sita, *J. Am. Chem. Soc.* **2001**, *123*, 6197–6198.
[16] K. C. Jayaratne, R. J. Keaton, D. A. Henningsen, L. R. Sita, *J. Am. Chem. Soc.* **2000**, *122*, 10490–10491.
[17] J. Richter, F. T. Edelmann, M. Noltemeyer, H.-G. Schmidt, M. Shmulinson, MS Eisen *J. Mol. Catal. A.* **1998**, *130*, 149–162.
[18] D. Walther, R. Fischer, H. Görls, J. Koch, B. Schweder, *J. Organomet. Chem.* **1996**, *508*, 13–22.
[19] R. Schlund, M. Lux, F. Edelmann, U. Reismann, W. Rohde, US6262198 to BASF Aktiengesellschaft, **2001**.
[20] S. Bambirra, M. W. Bouwkamp, A. Meetsma, B. Hessen, *J. Am. Chem. Soc.* **2004**, *126*, 9182–9183.
[21] B. J. O'Keefe, L. E. Breyfogle, M. A. Hillmyer, W. B. Tolman, *J. Am. Chem. Soc.* **2002**, *124*, 4384–4393.
[22] K. B. Aubrecht, K. Chang, M. A. Hillmyer, W. B. Tolman, *J. Polym. Sci. A: Polym. Chem.* **2001**, *39*, 284–293.
[23] F. A. Cotton, L. M. Daniels, J. H. Matonic, C. A. Murillo, *Inorg. Chim. Acta* **1997**, *256*, 277–282.
[24] F. A. Cotton, N. S. Dalal, C. Y. Liu, C. A. Murillo, J. M. North, X. Wang, *J. Am. Chem. Soc.* **2003**, *125*, 12945–12952.
[25] F. A. Cotton, L. M. Daniels, L. R. Falvello, J. H. Matonic, C. A. Murillo, *Inorg. Chim. Acta* **1997**, *256*, 269–275.
[26] F. A. Cotton, L. M. Daniels, C. A. Murillo, *Angew. Chem. Int. Ed. Engl.* **1992**, *31*, 737–738.
[27] F. A. Cotton, L. M. Daniels, C. A. Murillo, I. Pascual, H.-C. Zhou, *J. Am. Chem. Soc.* **1999**, *121*, 6856–6861.
[28] F. A. Cotton, C. A. Murillo, I. Pascual, *Inorg. Chem.* **1999**, *38*, 2182–2187.
[29] F. A. Cotton, L. M. Daniels, C. A. Murillo, *Inorg. Chem.* **1993**, *32*, 2881–2885.
[30] F. A. Cotton, X. Feng, C. A. Murillo, *Inorg. Chim. Acta* **1997**, *256*, 303–308.
[31] F. A. Cotton, L. M. Daniels, X. Feng, D. J. Maloney, J. H. Matonic, C. A. Murillo, *Inorg. Chim. Acta* **1997**, *256*, 291–301.
[32] F. A. Cotton, L. M. Daniels, D. J. Maloney, J. H. Matonic, C. A. Murillo, *Inorg. Chim. Acta* **1997**, *256*, 283–289.
[33] F. A. Cotton, L. M. Daniels, D. J. Maloney, C. A. Murillo, *Inorg. Chim. Acta* **1996**, *249*, 9- 11.
[34] S. Hao, S. Gambarotta, C. Bensimon, J. J. H. Edema, *Inorg. Chim. Acta* **1993**, *213*, 65–74.
[35] M. P. Coles, D. C. Swenson, R. F. Jordan, V. G. Young Jr., *Organometallics* **1997**, *16*, 5183–5194.
[36] A. R. Sadique, M. J. Heeg, C. H. Winter, *J. Am. Chem. Soc.* **2003**, *125*, 7774–7775.
[37] J. Cirera, P. Alemany, S. Alvarez, *Chem. Eur. J.* **2004**, *10*, 190–207.
[38] J. A. R. Schmidt, J. Arnold, *Chem. Commun.* **1999**, *1999*, 2149–2150.
[39] J. A. R. Schmidt, J. Arnold, *J. Chem. Soc., Dalton Trans.* **2002**, 2890–2899.
[40] J. A. R. Schmidt, J. Arnold, *Organometallics* **2002**, *21*, 2306–2313.
[41] J. A. R. Schmidt, J. Arnold, *J. Chem. Soc., Dalton Trans.* **2002**, 3454–3461.
[42] D. Abeysekera, K. N. Robertson, T. S. Cameron, J. A. C. Clyburne, *Organometallics* **2001**, *20*, 5532–5536.
[43] H. A. Jenkins, D. Abeysekara, D. A. Dickie, J. A. C. Clyburne, *J. Chem. Soc., Dalton Trans.* **2002**, 3919–3922.
[44] L. K. Johnson, C. M. Killian, M. Brookhart, *J. Am. Chem. Soc.* **1995**, *117*, 6414–6415.
[45] B. L. Small, M. Brookhart, A. M. A. Bennett, *J. Am. Chem. Soc.* **1998**, *120*, 4049–4050.
[46] G. J. P. Britovsek, V. C. Gibson, B. S. Kimberley, P. J. Maddox, S. J. McTavish, G. A. Solan, A. J. P. White, D. J. Williams, *Chem. Commun.* **1998**, 849–850.
[47] G. J. P. Britovsek, M. Bruce, V. C. Gibson, B. S. Kimberley, P. J. Maddox, S. Mastroianni, S. J. McTavish, C. Redshaw, G. A. Solan, S. Stromberg, A. J. P. White, D. J. Williams, *J. Am. Chem. Soc.* **1999**, *121*, 8728–8740.
[48] L. Bourget-Merle, M. F. Lappert, J. R. Severn, *Chem. Rev.* **2002**, *102*, 3031–3065.
[49] R. T. Boeré, V. Klassen, G. Wolmershauser, *J. Chem. Soc. Dalton Trans.* **1998**, 4147–4154.
[50] M. P. Coles, D. C. Swenson, R. F. Jordan, V. G. Young Jr., *Organometallics* **1998**, *17*, 4042–4048.
[51] B. S. Lim, A. Rahtu, J.-S. Park, R. G. Gordon, *Inorg. Chem.* **2003**, *42*, 7951–7958.
[52] H. Kawaguchi, T. Matsuo, *Chem. Commun.* **2002**, 958–959.
[53] B. Vendemiati, G. Prini, A. Meetsma, B. Hessen, J. H. Teuben, O. Traverso, *Eur. J. Inorg. Chem.* **2001**, 707–711.
[54] J. R. Hagadorn, J. Arnold, *Inorg. Chem.* **1997**, *36*, 132–133.
[55] D. Walther, P. Gebhardt, R. Fischer, U. Kreher, H. Görls, *Inorg. Chim. Acta* **1998**, *281*, 181–189.
[56] H. K. Lee, T. S. Lam, C.-K. Lam, H.-W. Li, S. M. Fung *New J. Chem.* **2003**, *27*, 1310–1318.
[57] F. A. Cotton, L. M. Daniels, C. A. Murillo, P. Schooler, *J. Chem. Soc., Dalton Trans.* **2000**, 2001–2005.

[58] J.-K. Buijink, M. Noltemeyer, F. T. Edelmann *Z. Naturforsch.* **1991**, *46b*, 1328–1332.
[59] R. D. Shannon *Acta Crystallogr. A.* **1976**, *32*, 751–767.
[60] P. N. Hawker, M. V. Twigg, "Iron(II) and Lower States", in: *Comprehensive Coordination Chemistry – The synthesis, reactions, properties & applications of coordination compounds*, Pergamon, Oxford, **1987**, p. 1179–1288.
[61] P. N. Hawker, M. V. Twigg, "Iron: Inorganic & Coordination Chemistry", in: *Encyclopedia of Inorganic Chemistry*, John Wiley & Sons, New York, **1994**, p. 1699–1725.
[62] A. Earnshaw, E. A. King, L. F. Larkworthy, *J. Chem. Soc. A* **1968**, 1048–1052.
[63] V. Esposito, E. Solari, C. Floriani, N. Re, C. Rizzoli, A. Chiesi-Villa, *Inorg. Chem.* **2000**, *39*, 2604–2613.
[64] J. P. Collman, J. L. Hoard, N. Kim, G. Lang, C. A. Reed, *J. Am. Chem. Soc.* **1975**, *97*, 2676–2681.
[65] H. Kalish, H. M. Lee, M. M. Olmstead, L. Latos-Grazynski, S. P. Rath, A. L. Balch, *J. Am. Chem. Soc.* **2003**, *125*, 4674–4675.
[66] B. W. Dale, R. J. P. Williams, C. E. Johnson, T. L. Thorp *J. Chem. Phys.* **1968**, *49*, 3441–3442.
[67] A. B. P. Lever, *J. Chem. Soc.* **1965**, 1821 –1829.
[68] B. W. Dale, *Mol. Phys.* **1974**, *28*, 503–511.
[69] C. G. Barraclough, R. L. Martin, S. Mitra, R. C. Sherwood *J. Chem. Phys.* **1970**, *53*, 1643–1648.
[70] T. J. Truex, R. H. Holm, *J. Am. Chem. Soc.* **1972**, *94*, 4529–4538.
[71] V. L. Goedken, Y.-A. Park *J. Chem. Soc. Chem. Commun.* **1975**, 214–215.
[72] S. Koch, R. H. Holm, R. B. Frankel, *J. Am. Chem. Soc.* **1975**, *97*, 6714–6723.
[73] D. P. Riley, J. A. Stone, D. H. Busch, *J. Am. Chem. Soc.* **1977**, *99*, 767–777.
[74] D. Sellmann, T. Becker, F. Knoch, *Chem. Ber.* **1996**, *129*, 509–519.
[75] D. Sellmann, U. Kleine-Kleffmann, L. Zapf, *J. Organomet. Chem.* **1984**, *263*, 321–331.
[76] A. Earnshaw *Introduction to magnetochemistry*, Academic Press Inc. Ltd., London, **1968**.
[77] C. J. O'Connor, "Magnetochemistry – Advances in Theory and Experimentation", in *Progress in Inorganic Cchemistry*, John Wiley & Sons, New York, **1982**, p. 203–283.
[78] R. Poli, *Chem. Rev.* **1996**, *96*, 2135–2204.
[79] R. R. Ernst, G. Bodenhausen, A. Wokaun, *Principles of Nuclear Magnetic Resonance in One and Two Dimensions*, Clarendon Press, Oxford, **1987**, p. 490.
[80] F. A. Carey, R. J. Sundberg, *Advanced Organic Chemistry, Part A: Structure and Mechanisms*, Plenum Press, New York, **1990**, p. 194.
[81] GAMESS-UK is a package of ab initio programs written by M. F. Guest, J. H. Van Lenthe, J. Kendrick, K. Schoffel, P. Sherwood, with contributions from R. D. Amos, R. J. Buenker, H. J. J. Van Dam, M. Dupuis, N. C. Handy, I. H. Hillier, P. J. Knowles, V. Bonacic-Koutecky, W. Von Niessen, R. J. Harrison, A. P. Rendell, V. R. Saunders, A. J. Stone, A. H. De Vries, the package is derived from the original GAMESS code due to M. Dupuis, D. Spangler, J. Wendoloski, NRCC Software Catalog, vol. 1, program no. QG01 (GAMESS), **1980**. DFT module by P. Young under the auspices of EPSRC's Collaborative Computational Project No. 1 (CCP1), **1995–1997**.
[82] P. Kovacic, N. O. Brace, *Inorg. Synth.* **1960**, *6*, 172–173.
[83] G. H. Cady, H. F. Holztclaw, J. Kleinberg, E. G. Rochow, W. C. Schumb, J. D. Scott, *Inorg. Synth.* **1957**, *5*, 153–156.
[84] L. G. L. Ward, *Inorg. Synth.* **1972**, *13*, 162–163.
[85] T. D. Goddard, D. G. Kneller, *SPARKY-V3.106*, University of California, San Francisco, **2003**.
[86] O. Kahn, *Molecular magnetism*; Wiley-VCH, New York, **1993**.
[87] SMART, SAINT, SADABS, XPREP and SHELXTL/NT: Area Detector Control and Integration Software, 2**000**; Smart Apex Software Reference Manuals; Bruker Analytical X-ray Instruments. Inc., Madison, Wisconsin, USA.
[88] G. M. Sheldrick, *SADABS-V2 – Multi-Scan Absorption Correction Program*, University of Göttingen, Göttingen, Germany, **2001**.
[89] A. J. M. Duisenberg *J. Appl. Crystallogr.* **1992**, *25*, 92–96.
[90] A. L. Speok *J. Appl. Crystallogr.* **1988**, *21*, 578–579.
[91] M. R. Snow, E. R. T. Tiekink, *Acta Crystallogr. B* **1988**, *44*, 676–677.
[92] Y. Le Page, *J. Appl. Crystallogr.* **1987**, *20*, 264–269.
[93] P. T. Beurskens, G. Beurskens, R. de Gelder, S. García-Granda, R. O. Gould, R. Israël, J. M. M. Smits, *The DIRDIF-99 Program System*, Crystallography Laboratory, University of Nijmegen, Nijmegen, The Netherlands, **1999**.
[94] A. Altomare, M. C. Burla, M. Camalli, G. L. Cascarano, C. Giacovazzo, A. Guagliardi, A. G. G. Moliterni, G. Polidori, R. Spagna, *J. Appl. Crystallogr.* **1999**, *32*, 115–119.
[95] A. Altomare, M. C. Burla, M. Camalli, G. L. Cascarano, C. Giacovazzo, A. Guagliardi, A. G. G. Moliterni, G. Polidori, R. Spagna, *SIR-97 – A Package for Crystal Structure Solution by Direct Methods and Refinement*, Univ. of Bari, Univ. of Perugia and Univ. of Roma, Italy, **1997**.
[96] *International Tables for Crystallography*, Kluwer Academic Publishers; Dordrecht, The Netherlands, **1992**.
[97] G. M. Sheldrick, *SHELXL-97 – Program for the refinement of crystal structures*, University of Göttingen, Göttingen, Germany, **2003**.
[98] A. L. Spek, *PLATON - Program for the Automated Analysis of Molecular Geometry (A Multipurpose Crystallographic Tool)*, University of Utrecht, Utrecht, The Netherlands, **2002**.
[99] A. L. Spek, *Acta Crystallogr. A* **1990**, *46*, C34–C34.
[100] C. Lee, W. Yang, R. G. Par, *Phys. Rev. B* **1988**, *37*, 785–789.
[101] A. D. Beck, *J. Chem. Phys.* **1993**, *98*, 1372–1377.
[102] A. D. Becke, *J. Chem. Phys.* **1993**, *98*, 5648–5652.
[103] J. S. Binkley, J. A. Pople, W. J. Hehre, *J. Am. Chem. Soc.* **1980**, *102*, 939–947.
[104] P. J. Hay, W. R. Wadt, *J. Chem. Phys.* **1985**, *82*, 270–283.
[105] W. R. Wadt, P. J. Hay, *J. Chem. Phys.* **1985**, *82*, 284–298.
[106] P. J. Hay, W. R. Wadt, *J. Chem. Phys.* **1985**, *82*, 299–310.

Received: January 28, 2005

